Spin dynamics in (110) GaAs quantum wells under surface acoustic waves

Odilon D. D. Couto, Jr.,* R. Hey, and P. V. Santos
Paul-Drude-Institut für Festkörperelektronik, Hausvogteiplatz 5-7, 10117 Berlin, Germany
(Received 23 July 2008; published 10 October 2008)

Long spin transport lengths (>60 μm) independent of temperature up to approximately 80 K are demonstrated in (110) GaAs quantum wells using surface acoustic waves (SAWs). Study of the dynamics of spins aligned along the [110] direction shows that, in addition to the intrinsic absence of the D'yakonov-Perel' spin-relaxation mechanism [Sov. Phys. Semicond. **20**, 110 (1986)], the Bir-Aronov-Pikus mechanism [Sov. Phys. JETP **42**, 705 (1976)] is also suppressed due to the type-II carrier confinement imposed by the SAW piezoelectric potential. Experimental evidence is provided for suppression of the spin relaxation via motional narrowing effects induced by the mesoscopic carrier confinement in narrow stripes along the SAW wave front, thus demonstrating the tuning of the spin-relaxation rates with the acoustic power.

DOI: 10.1103/PhysRevB.78.153305 PACS number(s): 72.25.Rb, 72.25.Dc, 72.25.Fe, 77.65.Dq

Semiconductor spintronics is receiving considerable attention due to potential applications in quantum information processing.[1] In order to achieve long-range spin transport, substantial effort has been devoted to the control of the mechanisms limiting spin coherence. In intrinsic GaAs quantum wells (QWs) at low temperatures, the most relevant ones are normally the D'yakonov-Perel' (DP) (Ref. 2) and the Bir-Aronov-Pikus (BAP) (Ref. 3) spin-relaxation mechanisms. The former arises from the lack of inversion symmetry. Due to the spin-orbit (SO) coupling, moving electrons experience a momentum-dependent effective magnetic field $\mathbf{B}_{SO}(\mathbf{k})$, which lifts the degeneracy of the spin states. The dependence of $\mathbf{B}_{SO}$ on electron momentum $\mathbf{k}$ leads to a distribution of spin precession frequencies and, consequently, to the relaxation of the average spin vector. BAP is caused by electron-hole (e-h) scattering, which leads to spin flip due to the exchange interaction.

Different approaches for controlling DP dephasing in GaAs QWs have been proposed and demonstrated, such as motional narrowing induced by doping,[4] spin confinement within mobile quantum dots,[5] and in narrow two-dimensional channels.[6–8] Crystal symmetry has also been explored, with the most impressive results being achieved in (110) GaAs QWs, where $\mathbf{B}_{SO}$ lies always along the growth (z) direction, thus suppressing DP scattering for z-oriented spins.[9–12] Control of the BAP scattering mechanism for photoexcited spins at low temperatures is more subtle due to the inherent presence of electrons and holes. It can, however, be achieved by doping[13] or by carrier confinement in type-II potentials.[14,15]

In this Brief Report, we investigate the spin-relaxation dynamics during transport by surface acoustic waves (SAWs) in (110) GaAs QWs. We show how the SAW fields considerably enhance the lifetime of spins photoexcited along the growth direction (to values exceeding 20 ns) and transport them with the acoustic velocity over distances exceeding 60 μm. The long lifetimes and transport lengths persist up to liquid nitrogen temperatures. The analysis of the spin dynamics under different temperature, illumination intensity, and acoustic power reveals that the long spin lifetimes are due to (i) suppression of the DP mechanism for z-oriented spins, (ii) inhibition of the BAP mechanism due to the type-II spatial separation between electrons and holes induced by the SAW piezoelectric potential, and (iii) lateral confinement of the spins within submicrometer-wide potential wires oriented along the SAW wave fronts. Interestingly, we found that the spin lifetime reduces at high acoustic powers. The latter is assigned to a structural inversion asymmetry (SIA) contribution to spin relaxation induced by the SAW moving strain and piezoelectric fields.

The experiments were carried out on an 18-nm-thick undoped GaAs QW with $Al_{0.3}Gal_{0.7}As$ barriers grown by molecular-beam epitaxy on a (110) GaAs substrate.[16] Rayleigh SAWs propagating along the $x\|[001]$ direction of the QW plane were generated by applying a radio-frequency (rf) signal to a focusing interdigital transducer (IDT),[17] which operates at an acoustic wavelength $\lambda_{SAW}=5.6$ μm (Fig. 1), corresponding to a frequency $f_{SAW}=514$ MHz. The acoustic beam is approximately 20 μm wide. A 500-nm-thick layer of ZnO (not shown in Fig. 1) was sputtered on the sample surface to enhance the amplitude of the SAW piezoelectric field.

In the optically detected spin transport measurements, a focused left circularly polarized laser ($\lambda_L=785$ nm) generates carriers with spins polarized along the $z\|[110]$ direction onto an ≈ 5 μm spot G on the SAW path, where the carriers are trapped and transported by the moving piezoelectric potential (Fig. 1). The photoluminescence (PL) emitted by the transported carriers along the SAW channel was recorded by a charge-coupled-device (CCD) camera. The electron–heavy

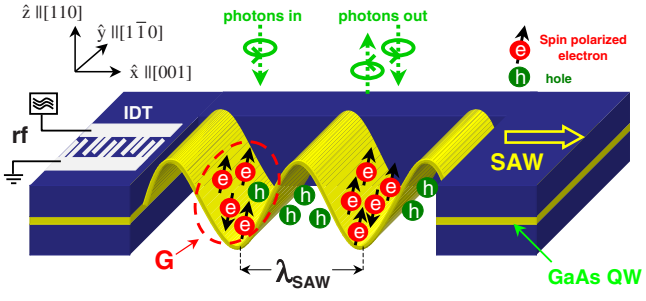

FIG. 1. (Color online) Acoustic transport mechanism: carriers are optically generated at a spot G and transported by the SAW. The degree of spin polarization of the electrons is obtained from the PL emitted along the transport path.

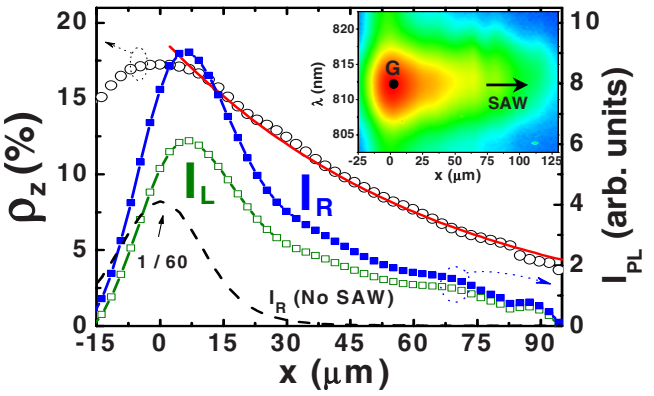

FIG. 2. (Color online) Spatial dependence of spin polarization ρ_z. The right vertical axis plots the intensities I_R and I_L for $P_{SAW}=58$ W/m integrated across the spectral width of the e-hh PL line along the transport channel shown in the inset. The dashed line shows I_R (divided by 60) for $P_{SAW}=0$.

hole (e-hh) PL line was spectrally selected using a monochromator and band-pass filters. By simultaneous detection of the right (I_R) and left (I_L) PL components, we determined the degree of spin polarization $\rho_z=(I_R-I_L)/(I_R+I_L)$.

The right vertical axis in Fig. 2 displays the spatial dependence of I_R and I_L integrated across the transport channel recorded at 15 K under a laser excitation power $P_{ex}=4$ μW. The dashed line shows I_R in the absence of a SAW, where the PL profile is determined by carrier diffusion and practically vanishes for $|x|\geq 20$ μm. A strong reduction in I_R (filled squares) and I_L (empty squares) by a factor of ≈ 30 (at $x=0$) takes place when a SAW with an effective acoustic power $P_{SAW}=58$ W/m is launched. The photogenerated carriers are transported over distances exceeding 120 μm away from G by the strong SAW piezoelectric potential (cf. PL micrograph in the inset). The I_R profile remains above the I_L one along the whole spatial range, demonstrating a nonzero electron-spin density in the channel (the hole spins relax much faster than the electron ones[15]). The circles in Fig. 2 (left vertical axis) display the spatial dependence of the spin polarization ρ_z, which decays exponentially (red solid line) with a remarkably large spin transport length of $L_s=64$ μm. The latter corresponds to a spin lifetime of $\tau_z=L_s/v_x=22$ ns, where $v_x=2930$ m/s is the SAW velocity.[12] The very long spin lifetime for z-oriented spins in (110) GaAs QWs is primarily attributed to the suppression of the DP relaxation mechanism.[9]

Figure 3(a) displays on a half-logarithmic scale the decay of the spin polarization for different values of P_{ex}. For $x>15$ μm (and for the whole spatial range for the lower light intensities), the spin-relaxation rates are essentially independent of P_{ex}, thus indicating that the long-range acoustic transport is not limited by the e-h exchange interaction due to the spatial separation of electrons and holes during transport. For high illumination intensity ($P_{ex}=10$ μW curve), ρ_z decays faster close to the generation spot ($x<15$ μm). The latter is attributed to the BAP mechanism induced by the screening of the SAW piezoelectric potential due to the larger concentration of carriers at G. As the carriers are taken away from the generation spot, BAP relaxation is virtually eliminated.

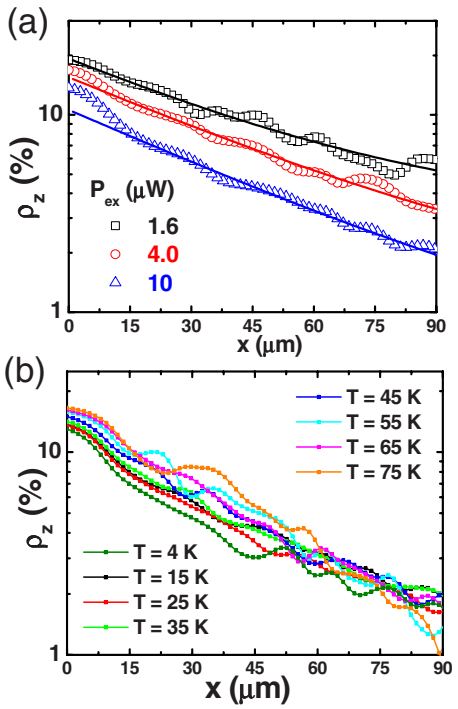

FIG. 3. (Color online) Decay of the spin polarization for different (a) light excitation powers P_{ex} (recorded at $T=15$ K using $P_{SAW}=14.6$ W/m) and (b) temperatures ($P_{SAW}=11.6$ W/m and $P_{ex}=4$ μW).

Figure 3(b) shows that the spin-polarization profiles are essentially independent of temperature (T) up to 75 K. The invariance of L_s with T further confirms the quenching of the BAP mechanism during acoustic transport since the reduction in the e-h correlation with temperature leads to an enhancement of spin lifetimes.[9,11] Reliable transport measurements could not be carried out above 80 K due to the reduced transport efficiency.

The dependence of the spin lifetime τ_z on P_{SAW} is shown in Fig. 4(a) (left vertical). The corresponding values of L_s (on the right) show an increase from 35 μm [for $P_{SAW}=5$ W/m] up to 65 μm [for $P_{SAW}=92$ W/m]. This result shows that the acoustic power can be used to tune the spin-relaxation rate. We note that the carrier transport length (obtained from the PL decay along the SAW path) is independent of P_{SAW} in this rf-power range, so that the enhanced spin transport lengths cannot be attributed to an increased carrier transport efficiency.

In the absence of BAP mechanism, the z component of the electron spin in (110) QWs becomes sensitive to weak in-plane effective magnetic fields, such as those arising from SIA contributions due to asymmetric confinement potentials induced by differences between the two QW interfaces.[10,14,18] These SIA effective magnetic fields slowly rotate the electron spin, thus adding an in-plane spin component. The D'yakonov-Perel' relaxation associated with this component leads to randomization of the average spin of the ensemble via carrier momentum fluctuations.[11,12] Spin relaxation due to such fluctuations can, however, be suppressed by scattering at mesoscopic potential boundaries[2] and, thus, be affected by the confinement induced by the strong SAW pi-

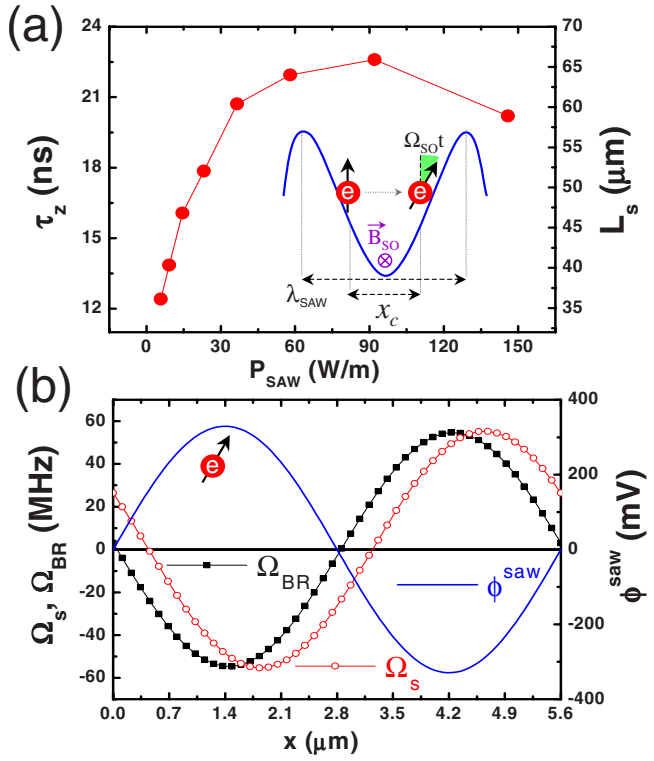

FIG. 4. (Color online) (a) Spin lifetimes (and the corresponding transport lengths on the right) as a function of P_{SAW}. The inset illustrates the electron-spin scattering in the confinement potential boundaries. (b) Larmor precession frequencies Ω_s and Ω_{BR} induced by the SAW strain and piezoelectric fields, respectively, over one SAW cycle for $P_{SAW}=140$ W/m. The right vertical axis shows the SAW piezoelectric potential.

ezoelectric potential. During acoustic transport, the carrier thermal velocity (v_T) is much higher than the SAW velocity ($v_T \gg v_x$). The enhancement of the SAW piezoelectric potential squeezes the electrons in potential wires, thus making the electron movement quasi-one-dimensional (parallel to the SAW wave front). As the acoustic power is increased (for $P_{SAW} \leq 90$ W/m) the momentum scattering rates of the electrons at the wire potential boundaries also increase, thus causing an enhancement of the in-plane spin component lifetime via motional narrowing effect.[2]

The effectiveness of the mesoscopic confinement for spin-relaxation suppression depends on the ratio between the confinement dimension (x_c) and the spin-orbit length (λ_{SO}) of the electron spins. λ_{SO} is defined as the ballistic transport distance required for a precession of the electron spin by an angle of 1 rad around the internal magnetic field $\mathbf{B}_{SO}(\mathbf{k})$ arising from the SO interaction. The suppression of spin relaxation via momentum scattering at the potential boundaries requires confinement dimensions much smaller than λ_{SO}. When the precession angle ($\Omega_{SO}t$) between two scattering events is very small, boundary scattering conserves the spin component, as illustrated in the inset of Fig. 4(a).

The SO length is given by the ratio $\lambda_{SO}=v/\Omega_{SO}$, where v is the electron velocity and Ω_{SO} the precession frequency around the SO field to which the spin component is sensitive. For the case of (110) QWs, when the initial z-spin component is rotated, the in-plane component becomes sensitive to the D'yakonov-Perel' internal magnetic field, which is oriented along the z direction. Using $v=\hbar k_y/m_0$ and $|\Omega_{SO}| = [\gamma \pi k_y / 2\hbar d_{eff}^2]$ (from Ref. 12), we obtain

$$\lambda_{SO} = \frac{2\hbar^2}{\gamma m_0}\left[\frac{d_{eff}}{\pi}\right]^2, \tag{1}$$

where m_0 is the electron effective mass, γ the GaAs spin-splitting constant, and d_{eff} the effective QW thickness given by the nominal one plus the wave-function penetration in the QW barriers. Note that Eq. (1) does not depend on the carrier momentum. Using $\gamma=18$ eV Å^3 (from Ref. 12) and assuming an effective QW thickness of $d_{eff}=20$ nm, Eq. (1) yields $\lambda_{SO}=5.2$ μm.

For acoustic transport, the average lateral carrier confinement length (x_c) depends on λ_{SAW} and on the amplitude of the SAW piezoelectric potential (ϕ^{SAW}). The sinusoidal spatial distribution of $\phi^{SAW}(x)=\phi_0 \cos(k_{SAW}x)$ can be approximated around the minimum of the electron energy (at $x=x_e$) by $\phi^{SAW}(x) \approx \frac{1}{2}\phi_0 k_{SAW}^2 (x-x_e)^2$, where ϕ_0 is the SAW piezoelectric potential amplitude and $k_{SAW}=2\pi/\lambda_{SAW}$. The average confinement distance can be estimated by

$$x_c = 2\sqrt{\langle (x-x_e)^2 \rangle} = \frac{\lambda_{SAW}}{\pi}\sqrt{\frac{2k_BT}{\phi_0}}, \tag{2}$$

with k_B as the Boltzmann constant. Using the numerical procedure described in Ref. 17, we calculate ϕ_0 expected for our multilayer structure.[16] Even for a low acoustic power of 5 W/m, we obtain $\phi_0=60$ mV, which at $T=15$ K corresponds to $x_c=0.35$ μm $\ll \lambda_{SO}$.

In the collision dominated regime, the electron-spin-relaxation rates can be affected by changes in the momentum scattering time $\tau_p (1/\tau_z \propto \tau_p)$,[10] which can be induced by changes in ϕ_0. The rise on the spin lifetimes with P_{SAW} observed in Fig. 4(a) can, therefore, be mainly attributed to the decrease in τ_p, which can be estimated by the ratio between x_c and v_T. We obtain $\tau_p \approx \lambda_{SAW}/\pi\sqrt{m_0/\phi_0}$. In the range of P_{SAW} from 5 to 60 W/m, ϕ_0 is calculated to lead to a relative decrease in τ_p by a factor of 1.9, which agrees reasonably well with the experimental variation of τ_z with P_{SAW} in this acoustic power range.

As the acoustic power is increased, the spin lifetime saturates and decreases for $P_{SAW} > 90$ W/m. This decrease for higher values of P_{SAW} is probably related to the spin relaxation induced by the moving SAW fields. A Rayleigh wave propagating along the [001] direction carries a strain and a piezoelectric field which reduce the QW symmetry and lead to SIA contributions to spin relaxation. It can be shown that the SAW-induced SIA contribution to spin relaxation for this Rayleigh wave is described by a Larmor frequency,

$$\Omega_{SAW} = \Omega_s + \Omega_{BR} = -\left[\frac{C_3 S_{xz}}{\hbar} + \frac{\alpha E_z}{\hbar}\right]\langle k_x \rangle \hat{y}. \tag{3}$$

Ω_{SAW} is always perpendicular to carrier propagation direction, i.e., along $\hat{y} \| [1\bar{1}0]$. The first term (Ω_s) corresponds to the Larmor frequency induced by the strain field, which is determined by the strain component S_{xz}.[19] The second term

describes the Bychkov-Rashba contribution to the spin splitting (Ω_{BR}) induced by the z component (E_z) of the SAW piezoelectric field.[17] $\langle k_x \rangle$ is the average carrier momentum determined by v_x, the SAW propagation velocity along [001]. C_3 and α are material specific parameters assumed to be 0.8 eÅ (Ref. 20) and 5.2 eÅ^2 (Ref. 21) for GaAs, respectively.

The amplitudes of Ω_s and Ω_{BR} along the SAW cycle obtained from the acoustic field distribution expected for $P_{SAW}=140$ W/m are displayed in Fig. 4(b). $\phi^{SAW}(x)$ is displayed in the right vertical axis. The minimum of the electronic energy $[-e\phi^{SAW}(x_e)]$, where the electrons are expected to be trapped ($x_e \approx 1.4$ μm), coincides with a location where the piezoelectric and strain-induced effective precession frequencies are close to their maximum amplitudes. A calculation for $P_{SAW}=140$ W/m yields a value of approximately 2 mT for the effective magnetic field experienced by the electrons during transport. Such field transforms the motional narrowing regime of the electron spins at low acoustic powers into a very slow precession motion around the average SAW-induced effective magnetic field. It is not shown but the spatial decay of ρ_z for $P_{SAW}=145.8$ W/m can, as expected, be reproduced with the anisotropic spin dephasing model[11,12] by using a magnetic field of 2 mT.

In conclusion, we have addressed the spin-relaxation mechanisms during long-range acoustic transport in a (110) GaAs QW. We showed that the piezoelectric potential of the SAW completely suppresses the BAP mechanism via quenching of the e-h interaction and also contributes to an enhancement of the spin lifetimes due to lateral confinement of the carriers. The spin transport lengths were shown to increase over tenths of microns without any significant changes with temperature up to 75 K. High acoustic fields, however, were shown to affect the spin-relaxation rates, providing perspectives for manipulation of moving spins by tuning the piezoelectric and strain fields of SAWs in future acoustic transport based spintronic devices.

We thank W. Seidel and M. Höricke for the growth and processing of the sample. Support from the Priority Program Spintronics from the DFG (Germany) is also acknowledged.

*odilon@pdi-berlin.de

[1] D. D. Awschalom and M. E. Flatté, Nat. Phys. **3**, 153 (2007).
[2] M. I. Dyakonov and V. Y. Y. Kachorovskii, Sov. Phys. Semicond. **20**, 110 (1986).
[3] G. L. Bir, A. G. Aronov, and G. E. Pikus, Sov. Phys. JETP **42**, 705 (1976).
[4] J. M. Kikkawa and D. D. Awschalom, Phys. Rev. Lett. **80**, 4313 (1998).
[5] J. A. H. Stotz, R. Hey, P. V. Santos, and K. H. Ploog, Nature Mater. **4**, 585 (2005).
[6] A. W. Holleitner, V. Sih, R. C. Myers, A. C. Gossard, and D. D. Awschalom, Phys. Rev. Lett. **97**, 036805 (2006).
[7] A. A. Kiselev and K. W. Kim, Phys. Rev. B **61**, 13115 (2000).
[8] A. G. Mal'shukov and K. A. Chao, Phys. Rev. B **61**, R2413 (2000).
[9] Y. Ohno, R. Terauchi, T. Adachi, F. Matsukura, and H. Ohno, Phys. Rev. Lett. **83**, 4196 (1999).
[10] O. Z. Karimov, G. H. John, R. T. Harley, W. H. Lau, M. E. Flatté, M. Henini, and R. Airey, Phys. Rev. Lett. **91**, 246601 (2003).
[11] S. Döhrmann, D. Hagele, J. Rudolph, M. Bichler, D. Schuh, and M. Oestreich, Phys. Rev. Lett. **93**, 147405 (2004).
[12] O. D. D. Couto, Jr., F. Iikawa, J. Rudolph, R. Hey, and P. V. Santos, Phys. Rev. Lett. **98**, 036603 (2007).
[13] T. Adachi, Y. Ohno, F. Matsukura, and H. Ohno, Physica E (Amsterdam) **10**, 36 (2001).
[14] K. C. Hall, K. Gündogdu, J. L. Hicks, A. N. Kocbay, M. E. Flatté, T. F. Boggess, K. Holabird, A. Hunter, D. H. Chow, and J. J. Zinck, Appl. Phys. Lett. **86**, 202114 (2005).
[15] T. Sogawa, P. V. Santos, S. K. Zhang, S. Eshlaghi, A. D. Wieck, and K. H. Ploog, Phys. Rev. Lett. **87**, 276601 (2001).
[16] R. Hey, A. Trampert, U. Jahn, O. D. D. Couto, Jr., and P. V. Santos, J. Cryst. Growth **301-302**, 158 (2007).
[17] M. M. de Lima, Jr. and P. V. Santos, Rep. Prog. Phys. **68**, 1639 (2005).
[18] L. S. Liu, W. X. Wang, Z. H. Li, B. L. Liu, H. M. Zhao, J. Wang, H. C. Gao, Z. W. Jiang, S. Liu, H. Cheng, and J. M. Zhou, J. Cryst. Growth **301-302**, 93 (2007).
[19] *Optical Orientation*, edited by F. Meier and B. P. Zakharchenya (North Holland, Amsterdam, 1984).
[20] V. Sih, H. Knotz, J. Stephens, V. R. Horowitz, A. C. Gossard, and D. D. Awschalom, Phys. Rev. B **73**, 241316(R) (2006).
[21] R. Winkler, *Spin-Orbit Coupling Effects in Two-Dimensional Electron and Hole Systems* (Springer, Berlin, 2003), Vol. 191.